Available online at www.sciencedirect.com

ScienceDirect

Mendeleev Commun., 2017, **27**, 623–625

Mendeleev Communications

Structural requirements for molecular design of positive allosteric modulators of AMPA receptor

Eugene V. Radchenko,[a,b] Dmitry S. Karlov,[a,b] Mstislav I. Lavrov[a,b] and Vladimir A. Palyulin*[a,b]

[a] *Department of Chemistry, M. V. Lomonosov Moscow State University, 119991 Moscow, Russian Federation. Fax: +7 495 939 0290; e-mail: vap@qsar.chem.msu.ru*

[b] *Institute of Physiologically Active Compounds, Russian Academy of Sciences, 142432 Chernogolovka, Moscow Region, Russian Federation*

DOI: 10.1016/j.mencom.2017.11.029

Positive allosteric modulators of AMPA receptor are prospective for the development of safe and efficacious agents for the correction of disruption of the central nervous system functions. Joint application of molecular docking, MFTA and CoMFA QSAR modelling, and pharmacophore analysis affords a consistent picture of structural requirements for molecular design of novel promising bivalent modulators with high activity, including overall twisted-staple shape of a molecule, hydrophobic central core, and polar hydrogen bond acceptor groups in peripheral parts of a molecule.

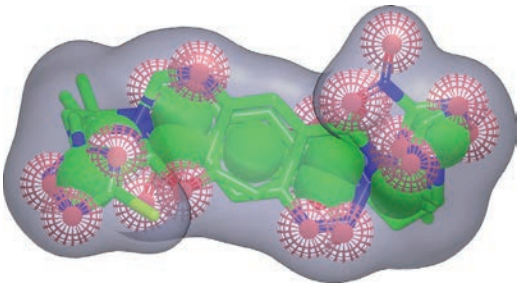

The glutamic acid is the major excitatory neurotransmitter in the mammalian brain. Among important types of the ionotropic glutamate receptors are the ligand-gated cation channels selectively activated by (*R*)-amino-3-hydroxy-5-methyl-4-isoxazolepropionic acid (AMPA) and involved in many important neurophysiological and neurological processes.[1,2] Thus, their positive allosteric modulators (PAMs), or 'ampakines', are prospective for the development of safe and efficacious neuroprotective agents,[3,4] cognition enhancers,[5,6] as well as drugs for treatment of the Alzheimer's disease,[7] major depression,[8] schizophrenia[9] and other conditions. The research in this field provided identification of several broad classes of compounds exhibiting PAM activity,[2,9] in particular, bivalent positive allosteric modulators of AMPA receptors possessing a record picomolar potency.[10] Significant advances in molecular modelling of the receptors and in elucidating the modulator structure–activity relationships have been achieved.[10–12] The aim of this work was to clarify the structural requirements for molecular design of AMPA receptor PAMs using the predictive QSAR and pharmacophore models derived from a representative series of modulators based on the polycyclic benzamide scaffold.

The training set containing the structures and the experimental PAM activity values for 141 compounds was built from the published data.[13–16] The appropriate best practices[17] ensuring the quality and consistency of the data were followed. The Instant JChem[18] software was used for the management and processing of the structure and activity data. The activity was characterized by the concentration of a compound EC_{2x} (mol dm^{-3}) that caused a twofold increase of the AMPA-induced neuronal current in a patch-clamp electrophysiological assay. In further analysis, the logarithmic values $pEC_{2x} = -\lg(EC_{2x})$ were used.

The QSAR models were built using two complementary methods: Molecular Field Topology Analysis (MFTA) and Comparative Molecular Field Analysis (CoMFA). The MFTA approach[19,20] aims to model the bioactivity in terms of local molecular descriptors (properties of atoms). The molecular supergraph constructed by topological alignment of structural formulas of the training set of compounds provides a common frame of reference for the meaningful comparison and analysis of local properties in different structures. The predictive QSAR models relating these properties in all positions of the molecular supergraph to the bioactivity were built using the partial least squares regression (PLSR) technique. The model predictivity was estimated by the fourfold cross-validation using the special stabilization procedure[20] which ensures the reliability and stability of the estimates, as well as prevents chance correlations even during the optimization of the descriptor set. The CoMFA approach[21] is a 3D QSAR technique that models the bioactivity in terms of steric and electrostatic interaction energies between the molecule and the probe species positioned in nodes of a rectangular grid. The ligand 3D structures were aligned according to the best molecular docking poses obtained by the FRED[22,23] software for the X-ray structure of the dimeric ligand-binding domain of AMPA receptor (PDB: 3RN8)[24] and the Omega-generated[25,26] ligand conformation library and additionally optimized using the SZIBKI[27] software (for each ligand, two poses reflecting the symmetry of the binding site were selected). The CoMFA models were built in the SYBYL-X[28] software using the Gasteiger–Hückel charges. The ROCS pharmacophore model (including the molecular shape and interaction centers) was derived from the same alignment using the vROCS[29,30] software.

The MFTA model was built for the training set comprising 111 compounds (compounds that have unreliable activity measurements and/or structures substantially different from the majority of the training set compounds were excluded). The structure of the molecular supergraph for this set of compounds and the examples of superimposition of training set structures are shown in Figure 1(*a*). The optimal model includes the following local molecular descriptors:[19,20] the effective atomic charge *Q* estimated by electronegativity equalization; the effective van der Waals radius of the first atomic environment R_e taking into account the steric requirements of a central non-hydrogen atom and other

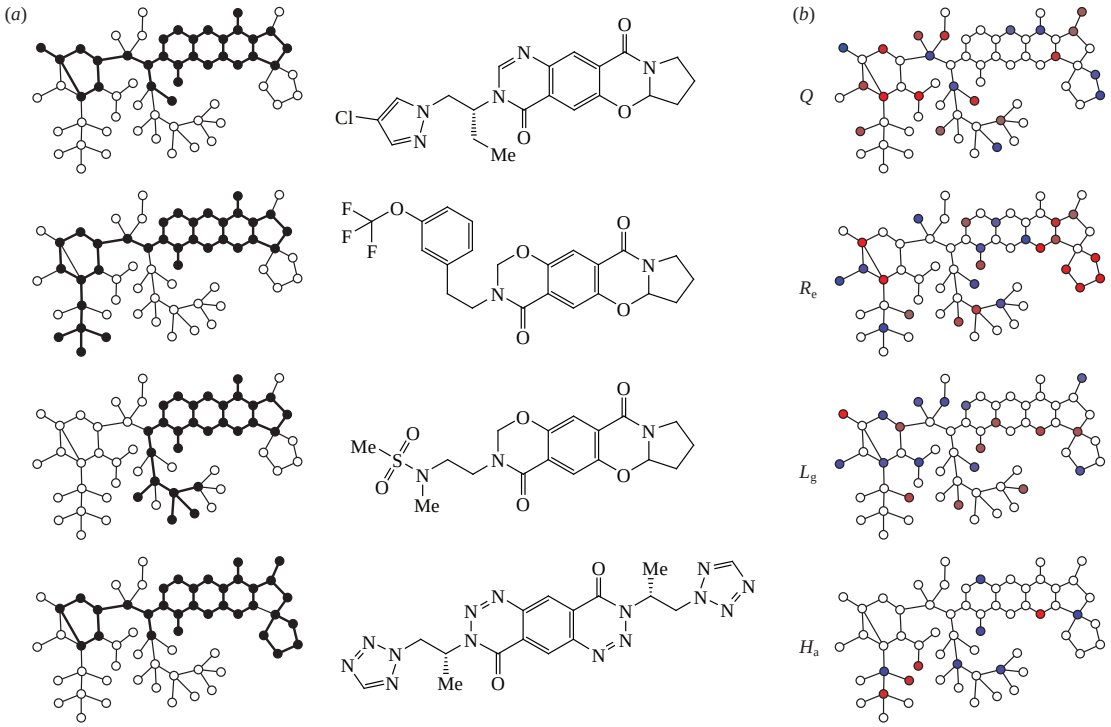

Figure 1 The MFTA model of PAM activity of polycyclic benzamides. (*a*) Molecular supergraph for the training set compounds with the examples of superimposition for four training set structures. (*b*) Activity maps representing the most significant effects of local descriptors on activity. In the positions marked with the red circles an increase in the descriptor values is favorable for the activity; conversely, in positions marked with the blue circles an increase in the descriptor values tends to decrease the activity. Intensity of colors reflects the magnitude of the influence. (For colour, refer to the online version of the article).

atoms attached to it; the group lipophilicity L_g taking into account the contributions of a central non-hydrogen atom and hydrogen atoms attached to it; and the ability of an atom to act as the hydrogen bond acceptor H_a. The influence of the hydrogen bond donor ability descriptors is not significant in this series. The model has the following statistical parameters: number of factors N_f = 5, squared correlation coefficient R^2 = 0.83, root mean square error RMSE = 0.43, cross-validation parameter Q^2 = 0.55 and root mean square error during cross-validation $RMSE_{cv}$ = 0.70. The activity maps shown in Figure 1(*b*) indicate the preference for aryl or hetaryl moieties with polar hydrogen bond acceptor substituents, as well as for moderately polar and/or lipophilic open-chain substituents.

The CoMFA model based on a subset of 49 benzotriazinone and benzopyrimidinone derivatives has the following statistical parameters: N_f = 4, R^2 = 0.75, RMSE = 0.47, Q^2 = 0.56. The CoMFA activity maps along with two docking poses of a training set structure **1** with the highest activity are shown in Figure 2. They are consistent with the MFTA conclusions and with the CoMFA model derived earlier[12] from the X-ray structures of the modulator–receptor complexes, as well as with the symmetrical structure of the PAM binding site shown in Figure 3. Note that the sterically favorable regions correspond to the subpockets formed by the Ile502, Pro515, Ser750, Lys751, Asn775 residues (hGluA2 numbering, UniProt: P42262) which are occupied by most of the high-activity ligands. The unfavorable regions correspond to clashes with the binding site residues such as Ser750 and Asn775. In some ligand positions, additional substituents may be introduced in order to enhance the binding. For example, based on a lead compound **1**, the structures **2** (illustrating possible modifications on the phenethyl moiety) and **3** (illustrating possible modifications on the pyrrolidine moiety) can be suggested.

The ROCS pharmacophore model derived from a subset of 15 compounds of very high activity ($pEC_{2x} \geqslant 8$) and based on three compounds **4**–**6** is shown in Figure 4. It provides good

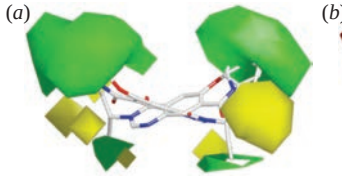

Figure 2 The CoMFA activity maps for the model of PAM activity of polycyclic benzamides. The two docking poses of a highest-activity training set structure **1** are shown for reference. (*a*) Steric influence map. In green-coloured regions additional steric bulk is favorable for activity and in yellow-coloured regions it is unfavorable. (*b*) Electrostatic influence map. In blue-coloured regions, the activity tends to be increased by additional positive charges, and in red-coloured regions by additional negative charges. (For colour, refer to the online version of the article).

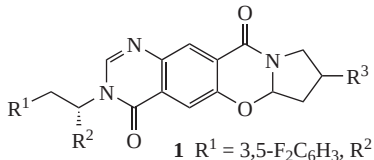

1 R^1 = 3,5-$F_2C_6H_3$, R^2 = C≡CH, R^3 = H
2 R^1 = 3-F-5-$NO_2C_6H_3$, R^2 = C≡CH, R^3 = H
3 R^1 = 3,5-$F_2C_6H_3$, R^2 = C≡CH, R^3 = OEt

4 R^1 = , R^2 = Me, R^3 = H

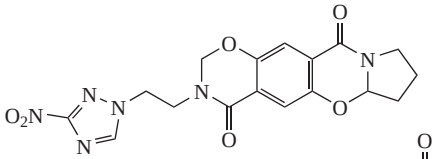

5

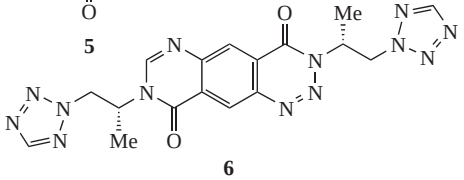

6

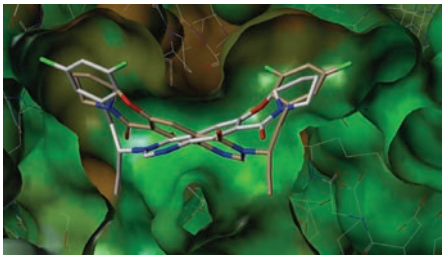

Figure 3 The PAM binding site at the dimer interface between ligand-binding domains of two AMPA receptor subunits (PDB: 3RN8). The protein Connolly surface is coloured according to the molecular lipophilic potential from brown for strongly hydrophobic regions to blue for strongly hydrophilic regions. The two docking poses of a high-activity structure **1** are represented by stick models. (For colour, refer to the online version of the article).

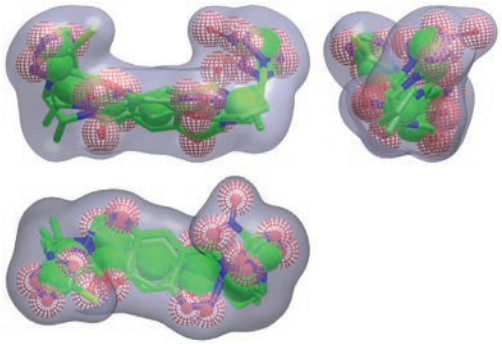

Figure 4 The ROCS pharmacophore model of polycyclic benzamides as positive allosteric modulators of AMPA receptor. Orthogonal projections are shown. The structures of the reference compounds **4**–**6** are represented by stick models. The shape of a sterically favourable region is shown in light gray, the green balls mark the positions of the centers of ring systems, and the pink mesh balls show the positions of the hydrogen bond acceptors. (For colour, refer to the online version of the article).

separation (AUCROC = 0.77) of the validation set containing 92 compounds with high ($pEC_{2x} \geqslant 7$) and low ($pEC_{2x} \leqslant 6$) activities. Similar to the MFTA and CoMFA models, it indicates that the modulator binding is primarily controlled by steric fit, by hydrophobic interactions with ring systems, and by hydrogen bond acceptors in peripheral parts of a molecule. The approximate C_2 symmetry of the model reflects the symmetry of the binding site. The overall twisted-staple shape of the sterically favorable region is consistent with earlier results.[12] For better binding, both binding site subpockets should be occupied. This can be achieved by combining the modifications illustrated by structures **2** and **3** as discussed above and/or by joining fragments of the ligands with a suitable angular linker based on a cage moiety.

In conclusion, joint application of molecular docking, MFTA and CoMFA QSAR modelling, and pharmacophore analysis provides a consistent picture of structural features required for high activity of bivalent positive allosteric modulators of AMPA receptor, including overall twisted-staple shape of a molecule, hydrophobic central core, and polar hydrogen bond acceptor groups in peripheral parts of a molecule. These results can be used to design novel promising modulator chemotypes.

We are grateful to the ChemAxon and OpenEye companies for kindly providing the academic licenses for the structural data processing and molecular modelling software. This work was supported by the Russian Science Foundation (grant no. 17-15-01455).

This article is dedicated to the memory of our colleague and mentor Professor Nikolay S. Zefirov (1935–2017).

References

1 S. F. Traynelis, L. P. Wollmuth, C. J. McBain, F. S. Menniti, K. M. Vance, K. K. Ogden, K. B. Hansen, H. Yuan, S. J. Myers and R. Dingledine, *Pharmacol. Rev.*, 2010, **62**, 405.
2 V. V. Grigoriev, A. N. Proshin, A. S. Kinzirsky and S. O. Bachurin, *Russ. Chem. Rev.*, 2009, **78**, 485 (*Usp. Khim.*, 2009, **78**, 524).
3 K. D. Destot-Wong, K. Liang, S. K. Gupta, G. Favrais, L. Schwendimann, J. Pansiot, O. Baud, M. Spedding, V. Lelièvre, S. Mani and P. Gressens, *Neuropharmacology*, 2009, **57**, 277.
4 E. B. Bloss, R. G. Hunter, E. M. Waters, C. Munoz, K. Bernard and B. S. McEwen, *Exp. Neurol.*, 2008, **210**, 109.
5 J. C. Lauterborn, L. C. Palmer, Y. Jia, D. T. Pham, B. Hou, W. Wang, B. H. Trieu, C. D. Cox, S. Kantorovich, C. M. Gall and G. Lynch, *J. Neurosci.*, 2016, **36**, 1636.
6 K. M. Partin, *Curr. Opin. Pharmacol.*, 2015, **20**, 46.
7 A. Tozzi, A. Sclip, M. Tantucci, A. de Iure, V. Ghiglieri, C. Costa, M. Di Filippo, T. Borsello and P. Calabresi, *Neurobiol. Aging*, 2015, **36**, 123.
8 R. Machado-Vieira, I. D. Henter and C. A. Zarate, Jr., *Prog. Neurobiol.*, 2017, **152**, 21.
9 S. E. Ward, L. E. Pennicott and P. Beswick, *Future Med. Chem.*, 2015, **7**, 473.
10 M. I. Lavrov, V. V. Grigor'ev, S. O. Bachurin, V. A. Palyulin and N. S. Zefirov, *Dokl. Biochem. Biophys.*, 2015, **464**, 322 (*Dokl. Akad. Nauk*, 2015, **464**, 626).
11 N. S. Zefirov and V. A. Palyulin, *Mendeleev Commun.*, 2010, **20**, 243.
12 D. S. Karlov, M. I. Lavrov, V. A. Palyulin and N. S. Zefirov, *Russ. Chem. Bull., Int. Ed.*, 2016, **65**, 581 (*Izv. Akad. Nauk. Ser. Khim.*, 2016, 581).
13 R. Mueller, Y.-X. Li, A. Hampson, S. Zhong, C. Harris, C. Marrs, S. Rachwal, J. Ulas, L. Nielsson and G. Rogers, *Bioorg. Med. Chem. Lett.*, 2011, **21**, 3923.
14 R. Mueller, S. Rachwal, M. E. Tedder, Y.-X. Li, S. Zhong, A. Hampson, J. Ulas, M. Varney, L. Nielsson and G. Rogers, *Bioorg. Med. Chem. Lett.*, 2011, **21**, 3927.
15 R. Mueller, S. Rachwal, S. Lee, S. Zhong, Y.-X. Li, P. Haroldsen, T. Herbst, S. Tanimura, M. Varney, S. Johnson, G. Rogers and L. J. Street, *Bioorg. Med. Chem. Lett.*, 2011, **21**, 6170.
16 R. Mueller, S. Rachwal, M. A. Varney, S. A. Johnson, K. Alisala, S. Zhong, Y.-X. Li, P. Haroldsen, T. Herbst and L. J. Street, *Bioorg. Med. Chem. Lett.*, 2011, **21**, 7455.
17 D. Fourches, E. Muratov and A. Tropsha, *J. Chem. Inf. Model.*, 2016, **56**, 1243.
18 *Instant JChem 17.3.27*, ChemAxon Ltd., 2017, http://www.chemaxon.com.
19 V. A. Palyulin, E. V. Radchenko and N. S. Zefirov, *J. Chem. Inf. Comp. Sci.*, 2000, **40**, 659.
20 E. V. Radchenko, V. A. Palyulin and N. S. Zefirov, in *Chemoinformatics Approaches to Virtual Screening*, eds. A. Varnek and A. Tropsha, Royal Society of Chemistry, Cambridge, 2008, pp. 150–181.
21 R. D. Cramer, D. E. Patterson and J. D. Bunce, *J. Am. Chem. Soc.*, 1988, **110**, 5959.
22 M. McGann, *J. Chem. Inf. Model.*, 2011, **51**, 578.
23 *OEDocking 3.2.0.2*, OpenEye Scientific Software, 2015, http://www.eyesopen.com.
24 D. E. Timm, M. Benveniste, A. M. Weeks, E. S. Nisenbaum and K. M. Partin, *Mol. Pharmacol.*, 2011, **80**, 267.
25 P. C. D. Hawkins, A. G. Skillman, G. L. Warren, B. A. Ellingson and M. T. Stahl, *J. Chem. Inf. Model.*, 2010, **50**, 572.
26 *OMEGA 2.5.1.4*, OpenEye Scientific Software, 2013, http://www.eyesopen.com.
27 *SZYBKI 1.9.0.3*, OpenEye Scientific Software, 2016, http://www.eyesopen.com.
28 *Sybyl-X 2.1*, Certara L.P., 2013, http://www.certara.com.
29 P. C. D. Hawkins, A. G. Skillman and A. Nicholls, *J. Med. Chem.*, 2007, **50**, 74.
30 *vROCS 3.2.1.4*, OpenEye Scientific Software, 2015, http://www.eyesopen.com.

Received: 18th July 2017; Com. 17/5310